

行政院國家科學委員會專題研究計畫 期中進度報告

以造膜理論控制左旋聚乳酸薄膜之裂解速度(1/2)

計畫類別：個別型計畫

計畫編號：NSC92-2216-E-002-014-

執行期間：92年08月01日至93年07月31日

執行單位：國立臺灣大學醫學工程學研究所

計畫主持人：楊台鴻

報告類型：精簡報告

報告附件：出席國際會議研究心得報告及發表論文

處理方式：本計畫可公開查詢

中 華 民 國 93 年 5 月 28 日



ELSEVIER

SCIENCE @ DIRECT®

Biomaterials ■ (■■■■) ■■■-■■■

Biomaterials

www.elsevier.com/locate/biomaterials

Preparation of PLLA membranes with different morphologies for culture of MG-63 Cells

Tai-Horng Young*, Hwa-Chang Liu, I-Chi Lee, Jyh-Horng Wang, Shu-Hua Yang Yang

Institute of Biomedical Engineering, College of Medicine, National Taiwan University, #1, Sec. 1 Jen-Ai Road, Taipei 100, Taiwan, ROC

Received 14 June 2003

Abstract

In this work, poly L-lactide (PLLA) membranes with different morphologies were prepared and the equilibrium phase diagram of membrane formation system of ethanol, methylene chloride, and PLLA was studied. Based on the phase diagram, particulate and porous membranes, dominated by crystallization and liquid–liquid demixing, respectively, could be prepared by changing the PLLA concentration of casting solution. In addition, in vitro interaction of MG-63 osteosarcoma cells and PLLA membranes with dense, porous and particulate morphologies was investigated. It was found that the particulate membrane not only could improve cell adhesion and growth, but also could upregulate the osteoblastic phenotype. Therefore, the PLLA membrane with particulate morphology satisfies the biomaterial requirement necessary for temporary scaffold to transplanted osteoblasts and provides a means for the architectural design of more complex tissue-engineered systems.

© 2003 Published by Elsevier Ltd.

Keywords: PLLA; Particulate membranes; MG-63 cells

1. Introduction

To design a scaffold for bone tissue engineering, a substrate is needed to guide cell adhesion, proliferation and differentiated function. Recently, biodegradable polymers are widely investigated in bone regeneration because of no need of a second surgical procedure to remove the device. Poly-L-lactide (PLLA), one of the few synthetic degradable polymers approved by the Food and Drug Administration (FDA) for certain human clinical applications, is a suitable substrate for osteoblasts cultures [1] and shows fracture healing results comparable to those of metallic implants [2,3]. Generally, most of PLLA substrates for osteoblasts culture have dense and smooth surface morphology. Since the biocompatibility of a substrate is also influenced by its surface morphology, salt-leaching technique has been used to generate porous morphology of biodegradable polymers to improve cell growth and new bone tissue formation [4,5]. Furthermore, Matsuzaka et al. showed that PLLA with microtextured

surfaces was able to influence the shape and the differentiation of osteoblasts-like cells [6]. Recognizing the importance of biomaterial surface morphology, a new surface morphology of PLLA substrate was prepared for culture of osteoblasts in this study. The substrate was characterized by a packed bed of nearly equal-diameter spherical particles that interconnected to form a special structure. In our previous studies, particulate morphology from other polymers such as polyamide, poly(vinylidene fluoride) (PVDF) and poly(ethylene-co-vinyl alcohol) (EVAL) has been shown to improve the biocompatibility of different cells [7–9]. However, it is still unknown how bone cells are stimulated by PLLA with particulate morphology. Therefore, the objective of this study was to prepare PLLA substrate with the particulate morphology and compare the responses of bone cells on the particulate morphology with traditional morphologies.

In this study, the PLLA substrates were used in the form of membranes. PLLA membranes with different surface morphologies were prepared by the phase inversion method [10]. The morphologies of PLLA membranes were investigated by scanning electron microscope (SEM). Human osteosarcoma MG-63 cells [11–13] were selected to evaluate the behaviors of bone

*Corresponding author. Tel.: +886-2231-23456; fax: +886-2239-40049.

E-mail address: thyoung@ha.mc.ntu.edu.tw (T.-H. Young).

cells on the prepared PLLA membranes. Here we measured, in addition to cell adhesion and cell growth examined by SEM and MTT assay, alkaline phosphatase (ALP) activity, as the differentiated function. The results of the investigation showed the particulate membrane provides a new surface morphology for improving the design and production of PLLA biomaterials intended for bone regeneration.

2. Materials and methods

2.1. Membrane preparation and characterization

An appropriate amount of PLLA (P-1566, Sigma, St. Louis, MO, USA) was dissolved in methylene chloride (MC, TEDIA DA-1431, Fairfield, OH, USA) to form a polymer solution at 25°C. Membranes were prepared by uniformly casting the polymer solution with a uniform thickness of about 300 µm on a glass plate, and then coagulated in an ethanol, extra pure reagent grade (Nacalai Tesque, Kyoto, Japan), bath at 25°C. After the precipitation was completed, the residual nonsolvent and solvent in the nascent membrane were removed by a series of washing steps. Subsequently, membranes were freeze-dried, then frozen in liquid nitrogen and fractured to expose the cross-sectional areas. The dried sample were gold coated and viewed with a SEM (S-800, Hitachi, Tokyo, Japan) at 20 kV. By changing the polymer concentration of the casting solution from 5 to 20 wt%, different membrane structures could be obtained [14,15].

The crystalline characteristics of each membrane were studied using a sensitive DSC 2010 (TA instruments, New Castle, Del, USA) under a nitrogen atmosphere. The temperature was raised from room temperature at a heating rate of 10°C/min to observe the endothermic peak of calorimetric transition. The melting temperature T_m is taken as the temperature at the maximum of the melting endotherm.

2.2. Phase diagram ethanol–MC–PLLA

In order to investigate the effect of the polymer concentration of the casting solution on the membrane structure, the phase diagram of ethanol–MC–PLLA was built, which is related to different types of phase separation during the membrane formation. The crystallization-induced gelation and liquid–liquid demixing boundaries were determined by cloud point method described in previous publications [16,17]. Briefly, a specific amount of dried PLLA polymer was mixed with a suitable amount of MC at 25°C until a clear homogeneous solution was obtained. Subsequently, this solution was blended with a known quantity of ethanol to prepare a series of solutions with different MC/

ethanol proportions. After a certain period, two types of phase-separated results could be observed: (i) solution precipitated into a white gel; and (ii) solution separated into two clear liquid layers. For case (i), the cloudy samples at these compositions are as a consequence of crystallization of PLLA molecules that have been proved by differential scanning calorimetry (DSC) in previous publications [16,17]. For case (ii), it is a typical liquid–liquid demixing. The crystallization-induced gelation and liquid–liquid demixing boundaries were determined as the composition at which phase separation began to occur in a series of samples.

2.3. Cell culture

The MG-63 cells derived from an osteosarcoma of a 14-year-old male (American Type Culture Collection, Rockville, MD, USA) were used in this study. The culture medium used was Dulbecco's modified Eagle's medium (DMEM) supplemented with 10% fetal calf serum (Gibco-RBL Life Technologies, Paisley, UK) and antibiotic/antimycotic (penicillin G sodium 100 U/ml, streptomycin 100 µg/ml, amphotericin B 0.25 µg/ml, Gibco-BRL Life Technologies, Paisley, UK). MG-63 cell lines were trypsinized using 0.1% trypsin and 0.1% ethylenediaminetetraacetic acid for 5 min, centrifuged at 400g for 5 min, and resuspended in the medium. For determination of the cell adhesion and cell growth, the prepared PLLA membranes with 15 mm in diameter were placed in 24-welled tissue culture polystyrene plates (Corning, Action, MA, USA). A silicon rubber ring 15 mm diameter was placed on each of the tested membranes in the wells to prevent them from floating. Membranes and silicon rubber rings were sterilized in 70% ethanol overnight and rinsed extensively with phosphate-buffered saline (PBS), followed by treatment under ultraviolet light overnight. Subsequently, 1 ml medium of cell suspension at a concentration of 2×10^5 cells/ml was added to each well and maintained in a humidified atmosphere with 5% CO₂ at 37°C. Cell suspension was also placed in empty tissue culture polystyrene dish (TCPS) with a silicon rubber ring as control groups. Control groups were treated the same as test membrane-containing wells.

2.4. Cell morphology

Cells adhering to the membranes were washed with PBS after 4 and 24 h incubation. Subsequently, the cells were fixed with 2.5% glutaraldehyde in PBS for 1 h at 4°C. The specimens, after being thoroughly washed with PBS, were dehydrated using graded ethanol changes, critical point dried, gold splattered in vacuum, and examined using SEM.

2.5. MTT assay

After cell culturing for 1 and 4 days, the viability of MG-63 cells was determined by MTT assay. The method of Mosmann [18] was modified and used in this study. MTT (M-2128, Sigma, St. Louis, MO, USA) was prepared as a 2 mg/ml stock solution in PBS, sterilized by Millipore filtration, and kept in dark. The 100 μ l of MTT solution was added to each well. After 3 h incubation at 37°C, 200 μ l of dimethyl sulfoxide (Nacalai Tesque, Kyoto, Japan) was added to dissolve the formazan crystals. The dissolvable solution was jogged homogeneously about 15 min by the shaker. The optical density of the formazan solution was read on an ELISA plate reader (ELx 800, BIO-TEK, Winooski, VT, USA) at 570 nm. The absorbance was proportional to the number of cells attached to the membrane surface [18].

2.6. Measurement of alp activity

ALP activity was measured spectroscopically by using an ALP kit (Diagnostic kit 104-LL, Sigma, St. Louis, MO, USA). Cell cultures were incubated for 1 and 4 days. After removal of the culture medium, cells were rinsed twice with PBS, and then lysed with 100 μ l of extraction buffer containing 2 mM MgCl₂ and 1% Triton X-100 in a shaker for 30 min at 37°C. Aliquots of 50 μ l were incubated with 100 μ l of *p*-nitrophenyl phosphate solution at 37°C for 30 min. The reaction was stopped using 100 μ l of 0.5 N sodium hydroxide, and the final absorbance was read on an ELISA plate reader at 405 nm. The calibration curve for ALP activity was made from the absorbance measurement of various concentrations of *p*-nitrophenol standard solution (Diagnostic kit 104-LL, Sigma, St. Louis, MO, USA),

which was measured in a similar manner as above. ALP activity was expressed as micromoles of reaction product (*p*-nitrophenol) per minute from a mg of cellular protein [19]. Protein concentration was determined, according to Smith et al. [20], with a commercially available assay bioassay kit (BCA protein assay, Pierce Chemical, Rockford, IL, USA). The absorbance at 570 nm was measured in an ELISA plate reader.

3. Results

3.1. Membrane morphology

Representative SEM photographs of PLLA membranes prepared with various PLLA concentrations of the casting solution are presented in Figs. 1–4. There are four sets of micrographs that cover the entire polymer-concentration range studied here. In Fig. 1, morphologies of the membrane are shown for the casting solution containing 20 wt% PLLA. Fig. 1(a) shows the top surface of this membrane is composed of particles of approximately 10 μ m in diameter. The connections of the membranes is from surface contact between particles. The fronts of these particles even impinge each other to form the polygonal structure with linear grain boundaries. Few voids left are the spaces resulting from incomplete coalescence of particles. Fig. 1(b) shows a structure formed of package of spherical particles in the cross section. Such a particulate morphology can be explained by the phase diagram of ethanol–MC–PLLA (shown in the next section).

When 15 wt% PLLA of the casting solution was employed, the membrane surface structure is similar to that prepared from the casting solution containing 20 wt% polymer, as shown in Fig. 2(a). This suggests

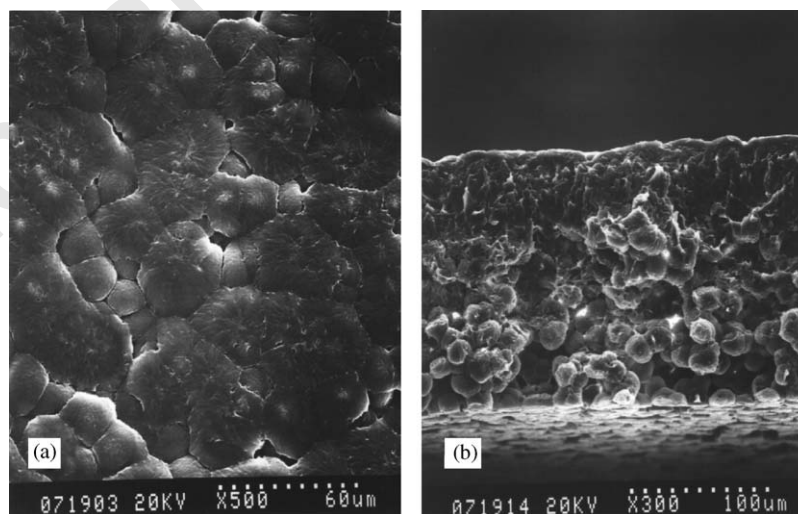


Fig. 1. SEM photographs of the PLLA membrane prepared with a casting solution containing 20 wt% PLLA: (a) top surface view; (b) cross-sectional view.

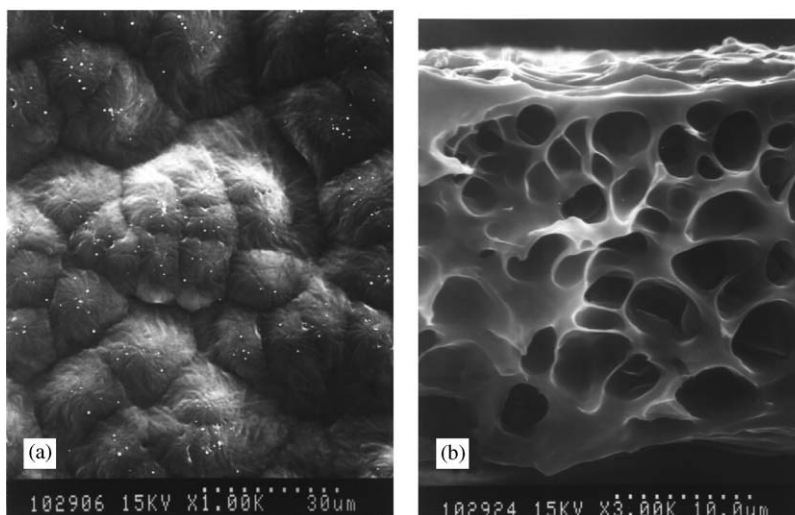


Fig. 2. SEM photographs of the PLLA membrane prepared with a casting solution containing 15 wt% PLLA: (a) top surface view; (b) cross-sectional view.

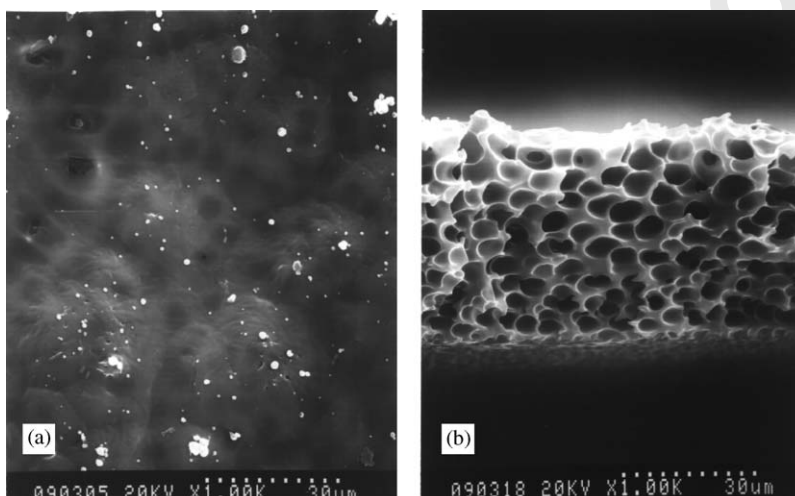


Fig. 3. SEM photographs of the PLLA membrane prepared with a casting solution containing 10 wt% PLLA: (a) top surface view; (b) cross-sectional view.

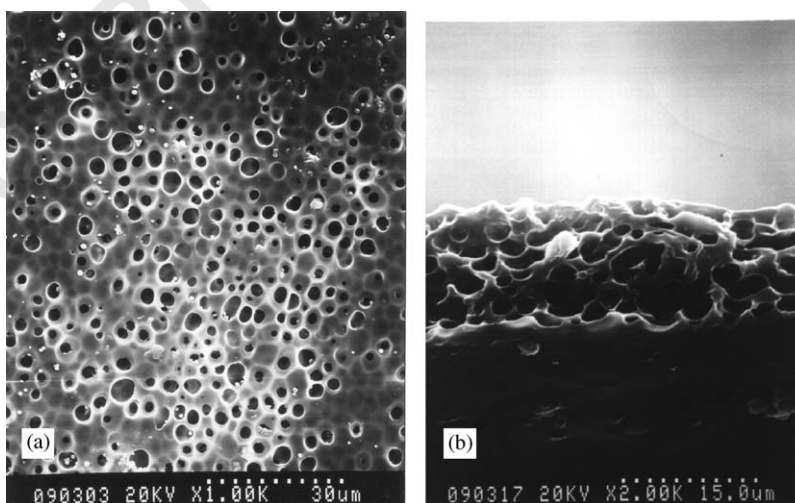


Fig. 4. SEM photographs of the PLLA membrane prepared with a casting solution containing 5 wt% PLLA: (a) top surface view; (b) cross-sectional view.

that the formation mechanism of membrane surface is identical in these two cases. However, a complete change in the structure of the cross section was observed, as shown in Fig. 2(b). The cross section of the membrane consists of irregular pores without particles existing in the cross section. Therefore, the effect of decreasing the PLLA concentration of the casting solution from 20–15 wt% on the membrane structure is only significant in the cross section.

When 10 wt% PLLA of the casting solution was employed, the structure of the membrane underwent dramatic changes. Unlike those observed in Figs. 1 and 2(a), the membrane surface shows fairly dense morphology without any particles existing (Fig. 3(a)). However, it can be noticed from a close look at the membrane surface that unclear pores located close to the membrane surface. Fig. 3(b) shows the cross section of the membrane consisted of cellular pores, which is similar to that obtained with 15 wt% PLLA of the casting solution.

In Fig. 4, morphologies of the membrane are shown for the casting solution containing 5 wt% PLLA. The membrane had a cellular surface (Fig. 4(a)) supported by a porous sublayer (Fig. 4(b)). Such a porous configuration is the so-called “sponge structure” that are produced by the liquid–liquid demixing process, similar to those of amorphous polymer membranes [21].

3.2. Phase diagram of ethanol–MC–PLLA

In Fig. 5, the phase diagram of ethanol–MC–PLLA at 25°C is shown. The triangular and circular symbols are, respectively, the composition at which gelation and two equilibrium liquid phases first occurs in a series of

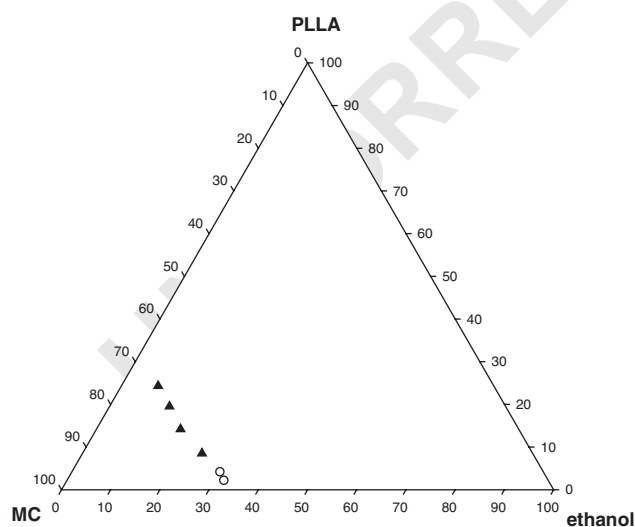


Fig. 5. Phase diagram of ethanol–MC–PLLA at 25°C. The data points, denoted by triangles (▲) and circles (○), represent the composition at which the gelation and two liquid phases first occurs in a series of samples with increasing ethanol concentration.

samples with increasing ethanol concentration. A solution at the MC-rich region is homogeneous and transparent. When the solution was above the gelation boundary, the solution underwent solid–liquid demixing to form a gel consisting of small polymer aggregates dispersed in a liquid phase. Basically, the aggregate was representative of crystallization from a homogeneous mixture as have also been observed for other semicrystalline polymers [16,17,22,23]. On the other hand, the crystallization-induced gelation disappeared as two equilibrium liquid phases at low polymer concentration region. This suggests that liquid–liquid demixing is favored to separate a dilute PLLA solution into two clear liquid phases. Therefore, using 5 wt% PLLA of the casting solution to prepare membranes, the membrane structure with porous morphology is controlled by liquid–liquid demixing. Conversely, a high concentrated PLLA solution prefers to undergo the solid–liquid demixing rather than the liquid–liquid demixing. Therefore, using 20 wt% PLLA of the casting solution to prepare membranes, the membrane structure with linking of particles is controlled by crystallization. Furthermore, the particles of this membrane are approximately equal size, suggesting that all of the particles emerged from individual PLLA nuclei are born simultaneously. These nuclei then grow radially until their fronts meet and join with adjacent particles.

3.3. DSC analysis

The DSC results of the prepared PLLA membranes are shown in Table 1. It appears that the melting temperatures present no discernible quantitative trend. Based on the data of heat of fusion, the membrane obtained from 20 wt% PLLA of the casting solution has a somewhat higher crystallinity than found for the membrane prepared from 5 wt% PLLA of the casting solution. This implies that although liquid–liquid demixing initiate the precipitation process and dominate the formed membrane morphology for 5 wt% PLLA of the casting solution, crystallization actually occurs in the membrane formation process. This may be due to the composition of the polymer-rich phase falling into the crystallization region after liquid–liquid demixing has occurred [21]. However, because growth of liquid pores have completed, the structure has largely been fixed.

Table 1
DSC data of PLLA membranes

wt % PLLA of the casting solution	Melting temperature (°C)	Heat of fusion (J/g)
20	177.8	49.0
15	176.4	47.5
10	176.3	47.0
5	177.1	47.0



Fig. 6. The surface morphology of a dense PLLA membrane prepared by directly evaporating a casting solution of 20 wt% PLLA.

Crystallization affects the ultimate membrane morphology only to an insignificant extent and crystallinity is slightly lower than that dominated by solid-liquid demixing process.

3.4. Cell morphology

Since the PLLA membrane structure is dependent on the polymer concentration in the casting solution, it is a good model to compare the effect of membrane surface structure on the cell responses. However, it is not possible to observe cells on the prepared membranes using light microscope due to poor optical transparency. Therefore, scanning electron micrographs of osteoblasts on the prepared membranes were studied to observe the cellular phenomenological behavior. Besides the particulate and porous membranes, the osteoblast response on the dense PLLA membrane was observed. The dense membrane was prepared by directly evaporating 20 wt% PLLA of the casting solution, as shown in Fig. 6.

Fig. 7 shows the morphology of MG-63 cells attached on the various surface of PLLA membranes after

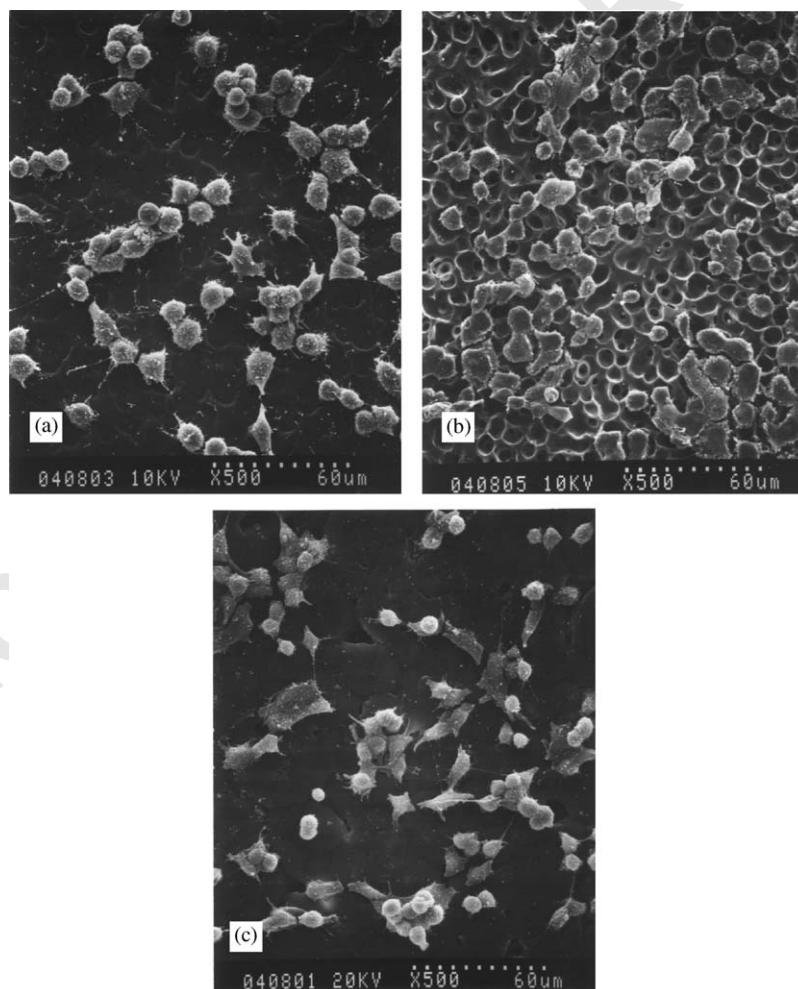


Fig. 7. SEM photographs of MG-63 cells cultured on the (a) dense, (b) porous, (c) particulate PLLA membranes after 4 h incubation.

1 cultured for 4 h. Surface morphology was significantly
2 found to influence the cell attachment. During the first
3 4 h in culture, MG-3 cells show a mixed morphology
4 between spherical and spread. It can be seen that the
5 principal morphology of cells on the dense surface of
6 membrane is just only in initial adhesion stage. As
7 shown in Fig. 7(a), SEM examination reveals that most
8 of cells are spherical in appearance. Fig. 7(b) shows the
9 morphology of MG-63 cells cultured on the surface of
10 porous membrane (prepared from 5 wt% PLLA of the
11 casting solution). It seems cells have comparable
12 adhesion characteristics on dense and porous mem-
13 branes. In contrast, the surface of the particulate
14 membrane (prepared from 20 wt% PLLA of the casting
15 solution) has different effects on the MG-63 cells. As
16 shown in Fig. 7(c), both spherical and spread morpho-
17 logies are observed. Clearly, the degree of cell spreading
18 on the particulate surface is higher than those observed
19 on dense and porous surfaces at the same time.
20 Qualitatively, the particulate membrane is more favor-
21 able for culture of MG-63 cells than the other two types

of membranes. Exactly what stimuli are responsible for
2 the observed phenomenon remains to be determined.
3 However, it is reasonable to attribute the difference in
4 cell adhesion to the PLLA membranes with different
5 surface morphologies.

6 Fig. 8 shows the morphology of MG-63 cells cultured
7 on three types of membranes for 1 day. Following the
8 initial stage of cell attachment, cells on the dense surface
9 of PLLA membrane undergo a change in morphology,
10 from a rounded shape to cytoplasmic extension (see Fig.
11 8(a)). In contrast, cells on the porous and particulate
12 membrane can be considered completely flattened and
13 well spread (Figs. 8(b) and (c)). At this time, cells grow
14 equally well and the stage of cell fusion is found to form
15 a monolayer on these two membranes. In addition, the
16 SEM pictures seem to reveal that the cell number of
17 dense membrane is less than that on the particulate
18 membrane. However, one has to be careful while making
19 this conclusion from SEM pictures since the selection of
20 the view from a microscope certainly changes the cell
21 number on the membrane. Nevertheless, the difference of

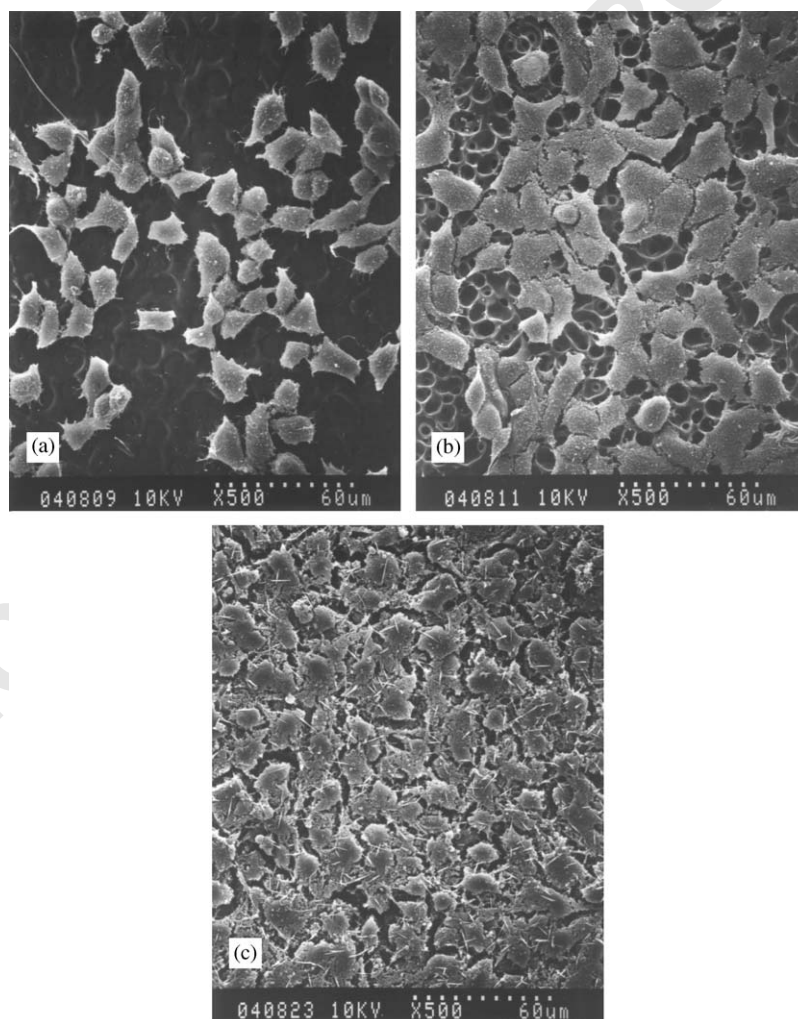


Fig. 8. SEM photographs of MG-63 cells cultured on the (a) dense, (b) porous, (c) particulate PLLA membranes after 1 d incubation.

the cell number between these two membranes is so clear that obviously the effect of membrane surface morphology remains observable, which will be confirmed by MTT assay and described in the next section.

3.5. MTT assay

The results in Fig. 9 depict the MTT conversion of cells attached to three types of membranes after 1 and 4 days in culture, which was determined from the ratio of the MTT conversion of cells attached to the PLLA membranes to that of cells attached to TCPS. The MTT assay relies on the ability of the viable cells to reduce a water-soluble yellow dye to a water-insoluble purple formazan product. The MTT value thus obtained is directly proportional to the cell number in each well [18]. Fig. 9 indicates that MG-63 cells on all the PLLA membranes are able to convert the MTT into a blue formazan product, regardless the membrane surface morphology. After 1 day of incubation, MTT counts of cells is similar for the particulate and porous membranes but greater compared with the dense membrane, which correlates with the obvious morphological differences of MG-63 cells and the cell number on these membranes by SEM observation (Fig. 8). After 4 days of incubation, MTT counts of cells attached to the dense membrane is significantly less than those attached to the particulate and porous membranes ($p < 0.05$). It is noted that the particulate membrane has the highest MTT counts after 4 days of incubation. Therefore, the particulate PLLA membrane is considered to be more favorable for proliferation of osteoblasts.

3.6. ALP activity

ALP activity, a parameter of bone cell differentiation, was measured for MG-63 cells cultured on three types of

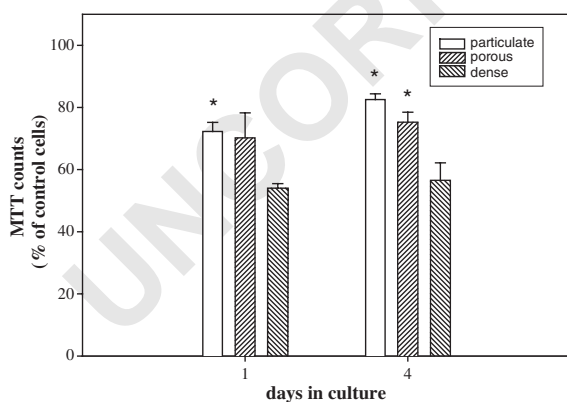


Fig. 9. MTT assay. Formazan absorbance of MG-63 cells attached to three types of membranes 1 and 4 days after cell seeding, $n = 4-6$. Data are presented as the mean \pm standard deviation. Asterisk denotes significant differences ($p < 0.05$) of formazan absorbance compared to the dense membrane, which was calculated using one-way analysis of variance (ANOVA) followed by Student's t -test.

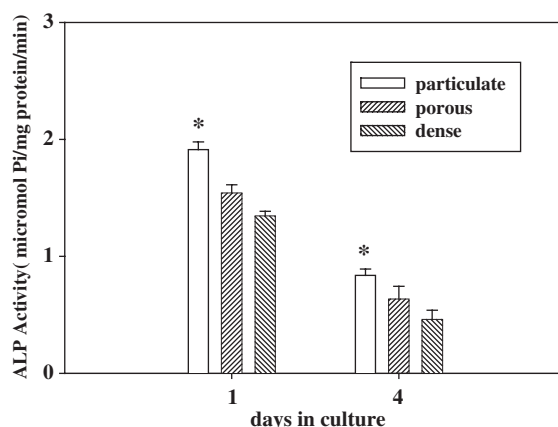


Fig. 10. ALP activity expressed by MG-63 cells cultured on three types of PLLA membranes after 1 and 4 days in culture, $n = 4-6$. Data are presented as the mean \pm standard deviation. Asterisk denotes significant differences ($p < 0.05$) of ALP activity compared to the dense membrane, which was calculated using one-way analysis of variance (ANOVA) followed by Student's t -test.

membranes for 1 and 4 days. Fig. 10 shows cells grown on all the membranes tested in this study express ALP activity decreased with culture time. Many cell types exhibit an inverse relationship between growth and differentiation in vitro [24]. Based on the results of Figs. 9 and 10, MG-63 cells cultured on three types of PLLA membranes exhibit a decrease in ALP activity simultaneously with an increase in the rate of cell proliferation. Therefore, our results are in accordance with studies by Quarles et al. [25], who observed that proliferating osteoblasts decreased production of ALP during periods of growth. However, similar to the results of MTT assay, the particulate membrane has the highest ALP activity, regardless of whether 1 or 4 days after culture is examined. Compared with the dense membrane, there are significant increases of 45% and 47% in ALP activity after 1 and 4 days of culture, respectively.

4. Discussion

In this article PLLA membranes with dense, porous and particulate morphologies were easily prepared by the phase inversion method and the behavior of MG-63 cells on these PLLA membranes were compared. Based on the analysis of the phase diagram (Fig. 5), porous and particulate membranes are controlled by liquid-liquid demixing and crystallization, respectively. Interestingly, besides PLLA, particulate membranes also can be prepared from other crystallizable polymers such as polyamide, PVDF and EVAL [8]. In our laboratory, such particulate membranes have been proved useful in plasma protein separation [26], microfiltration [27] and improving the biocompatibility of different cells [7-9]. However, prior to this study, very little was known about the characteristics of osteoblasts behavior on the

1 particulate PLLA membrane. PLLA was selected
2 because it is a biodegradable polymer and has been
3 approved by the FDA.

4 Our results clearly demonstrate that the membrane
5 surface morphology is an important factor for adhesion
6 and growth of MG-63 cells. Although cell attachment
7 occurs on three types of membranes, SEM studies show
8 that cells on the dense and porous membranes are able
9 to attach but unable to follow this attachment with
10 spreading during the first 4 h in culture. Qualitatively,
11 cells on the particulate membrane having a flatter and
12 spread shape at the same time. Moreover, it has been
13 demonstrated that cell proliferation on the particulate
14 membrane is significantly improved over that on the
15 dense membrane after 4 days of incubation, which
16 shows the particulate membrane is suitable for osteo-
17 blast seeding and growth. More importantly, the seeded
18 cells on the particulate membrane show more ALP
19 activity than cells on the other two types of membranes
20 through the experimental period.

21 Cell–biomaterial interaction is a very complicated
22 phenomenon and depends in a very sensitive manner on
23 the surface structure of biomaterials. Matsuzaka et al.
24 showed that microtextured surfaces are able to influence
25 the differentiation of osteoblasts-like cells [6]. However,
26 in this study, we provide a very easy way to produce a
27 new PLLA surface for osteoblasts culture. We believe
28 that this is the first time that the particulate PLLA
29 membrane has been used as a substrate for cell cultures
30 to examine its effect on cell response in vitro.

31 Overall, the MG-63 cells do respond better to the
32 particulate membrane. Exactly what factors are respon-
33 sible for culturing cells on the particulate membranes is
34 not clear. Obviously, some direct influence of the surface
35 particles on the cells must be involved. Although the
36 direct contact between cell and the substrate is the first
37 step for cell adhesion onto the substrate, it is known
38 cell–substrate adhesion is generally considered to be a
39 multi-step process involving adsorption of protein,
40 particularly components of the extracellular matrix
41 (ECM), such as fibronectin, laminin, and collagen, onto
42 the substrate surface and recognition of ECM compo-
43 nents by cell surface receptors, followed by cytoskeletal
44 rearrangements that lead to cell spreading [28]. Hence, a
45 possible explanation for the particulate membrane being
46 more favorable for the cell culture is that specific ECM
47 proteins may be adsorbed well on the rough membrane
48 surface, which not only causes a different preferential
49 accumulation of proteins, but also influences the
50 configuration of proteins. This indicates that the
51 protruding particles could provide a local three-dimen-
52 sional environment for adhesion and growth of MG-63
53 cells.

54 Besides surface structure is changed during the
55 membrane formation process, we cannot completely
exclude that differences in crystallization among three

types of membranes cause a different cell response. In
general, the effect of polymer crystallization on the cell
behavior is not clear but polymer crystallization can
decrease its degradation rate. Therefore, a thorough
study of the effects of polymer surface morphologies on
the biodegradation rate are under way and will be
reported separately in the near future. In fact, this paper
is the first paper of a series studies to study new surface
morphology for improving the design and production of
PLLA biomaterials intended for bone regeneration.
Animal studies will also be performed to evaluate the
healing and regeneration of bone on the particulate
PLLA membranes for a longer period.

In conclusion, the main finding of this study is the
feasibility of culturing osteoblastic cells on the particu-
late PLLA membrane. The particulate membrane not
only can improve cell adhesion and growth, but also can
upregulate the osteoblastic phenotype. Together with
our unpublished data that particulate structure indeed
can decrease the degradation rate of PLLA, thus, it has
the potential to make use of the particulate PLLA
membrane to improve the design and production of
PLLA biomaterials intended for bone regeneration.

Acknowledgements

The authors thank the National Taiwan University
Hospital and the National Science Council of the
Republic of China for their financial support.

References

- [1] Ishaug SL, Yaszemski MJ, Bizios R, Mikos AG. Osteoblast function on synthetic biodegradable polymers. *J Biomed Mater Res* 1994;28:1445–53.
- [2] Majola A, Vainionpaa S, Vihtonen K, Mero M, Vasenius J, Tormala P, Rokkanen P. Absorption, biocompatibility, and fixation properties of polylactic acid in bone tissue: an experimental study in rats. *Clin Orthop Rel Res* 1989;268:260–9.
- [3] Pihlajamaki H, Bostman O, Manninen M, Paivarinta U, Rokkanen P. Tissue-implant interface at an absorbable fracture fixation plug made of polylactic in cancellous bone of distal rabbit femur. *Arch Orthop Trauma Surg* 1994;113:101–5.
- [4] Attawia MA, Herbert KM, Laurencin CT. Osteoblast-like cell adherence and migration through 3-dimensional porous polymer matrices. *Biochem Biophys Res Commun* 1995;213:639–44.
- [5] Ishaug SL, Crane GM, Miller MJ, Yasko AW, Yaszemski MJ, Mikos AG. Bone formation by three-dimensional stromal osteoblast culture in biodegradable polymer scaffolds. *J Biomed Mater Res* 1997;36:17–28.
- [6] Matsuzaka K, Walboomers XF, deRuijter Je, Jansen JA. The effect of poly L-lactic acid with parallel surface micro groove on osteoblasts-like cells in vitro. *Biomaterials* 1999;20:1293–301.
- [7] Young TH, Lin CW, Cheng LP, Hsieh CC. Preparation of EVAL membranes with smooth and particulate morphologies for neuronal culture. *Biomaterials* 2001;22:1771–7.

- 1 [8] Young TH, Lin DT, Chen LY. Human monocyte adhesion and
activation on crystalline polymers with different morphology and
3 wettability in vitro. *J Biomed Mater Res* 2000;50:490–8.
- 5 [9] Young TH, Yao CH, Sun JS, Lai CP, Chen LW. The effect of
morphology variety of EVAL membranes on the behavior of
7 myoblasts in vitro. *Biomaterials* 1998;19:717–24.
- 9 [10] Kesting RE. *Synthetic polymeric membranes*. New York: Wiley;
1985.
- 11 [11] Kieswetter K, Schwartz Z, Hummert TW, Cochran DL, Simpson
J, Dean DD, Boyan BD. Surface roughness modulates the local
13 production of growth factors and cytokines by osteoblast-like
MG-63 cells. *J Biomed Mater Res* 1996;32:55–63.
- 15 [12] Kue R, Sohrabi A, Nagle D, Frondoza C, Hungerford D.
Enhancement proliferation and osteocalcin production by human
17 osteoblast-like MG-63 cells on silicon nitride ceramic discs.
Biomaterials 1999;20:1195–201.
- 19 [13] Wang JH, Wei CW, Liu HC, Young TH. Behavior of MG-63 cells
on nylon/chitosan-blended membranes. *J Biomed Mater Res*
2003;64A:606–15.
- 21 [14] van de Witte P, Esselbrugge H, Dijkstra PJ, van den Berg JWA,
Feijen J. Phase transitions during membrane formation of
23 polylactides. I. A morphological study of membranes obtained
from the system polylactide–chloroform–methanol. *J Membr. Sci*
1996;113:223–36.
- 25 [15] van de Witte P, Esselbrugge H, Dijkstra PJ, van de Berg JWA,
Feijen J. A morphological study of membranes obtained from the
27 systems polylactide–dioxane–methanol, polylactide–dioxane–
water, and polylactide–N–methyl pyrrolidone–water. *J Polym
Sci: Part B; Polym Phys* 1996;34:2569–78.
- 29 [16] Young TH, Lai JY, Yu WM, Cheng LP. Equilibrium phase
behavior of the membrane forming water–DMSO–EVAL copolymer
system. *J Membrane Sci* 1997;128:55–65.
- [17] Young TH, Cheng LP, Hsieh CC, Chen LW. Phase behavior of
EVAL polymer in water–2-propanol Cosolvent. *Macromolecules*
1998;31:1229–35.
- [18] Mosmann T. Rapid colorimetric assay for cellular growth and
survival: application of proliferation and cytotoxicity assays. *J
Immunol Methods* 1983;65:55–63. 31
- [19] Beck GR, Sullivan EC, Moran E, Zerler B. Relationship between
alkaline phosphatase levels, osteopontin expression, and miner-
33 alization in differentiating MC3T3-E1 osteoblasts. *J Cell Biochem*
1998;68:269–80. 35
- [20] Smith PK, Krohn RI, Hermanson GT, Mallia Ak, Gartner FH,
Provenzano MD, Fujimoto EK, Goeke NM, Olson BJ, Klenk
37 DC. Measurement of protein using bicinchoninic acid. *Anal
Biochem* 1985;150:76–85. 39
- [21] Cheng LP, Young TH, You WM. Formation of crystalline EVAL
membranes by controlled mass transfer process in water–DMSO–
41 EVAL copolymer systems. *J Membr Sci* 1998;145:77–90. 41
- [22] Lloyd DR, Kinzer KE, Tseng HS. Microporous membrane
formation via thermally induced phase separation. I. solid–liquid
43 phase separation. *J Membrane Sci* 1990;52:239–61. 43
- [23] Cheng LP, Young TH, Fang L, Gau JJ. Formation of particulate
microporous PVDF membranes by isothermal immersion pre-
45 cipitation from ethanol/dimethylformamide/PVDF system. *Poly-
mer* 1999;40:2395–403. 47
- [24] Mooney D, Hansen L, Vacanti J, Langer R, Farmer S, Ingber D.
Switching from differentiation to growth in hepatocytes: control
49 by extracellular matrix. *J Cell Phys* 1992;151:497–505. 49
- [25] Quarles LD, Yohay DA, Lever LW, Caton R, Wenstrup RJ.
Distinct proliferative and differentiated stages of murine MC3T3-
51 E1 cells in culture: an in vitro model of osteoblasts development. *J
Bone Miner Res* 1992;7:683–92. 53
- [26] Lin DT, Cheng LP, Kang YJ, Chen LW, Young TH. Effects of
precipitation conditions on the membrane morphology and
55 permeation characteristics. *J Membr Sci* 1998;140:185–94. 55
- [27] Young TH, Cheng LP, Lin HY. Interesting behavior for filtration
of macromolecules through EVAL membranes. *Polymer*
2000;41:377–83. 57
- [28] Grinnell F. Cellular adhesiveness and extracellular substrata. *Int
Rev Cytol* 1978;53:65–114. 59